Thioredoxin-dependent disulfide bond reduction is required for protamine eviction from sperm chromatin

Alexander V. Emelyanov and Dmitry V. Fyodorov

Albert Einstein College of Medicine, Department of Cell Biology, Bronx, New York 10461, USA

Cysteine oxidation in protamines leads to their oligomerization and contributes to sperm chromatin compaction. Here we identify the *Drosophila* thioredoxin Deadhead (DHD) as the factor responsible for the reduction of intermolecular disulfide bonds in protamines and their eviction from sperm during fertilization. Protamine chaperone TAP/p32 dissociates DNA–protamine complexes in vitro only when protamine oligomers are first converted to monomers by DHD. *dhd*-null embryos cannot decondense sperm chromatin and terminate development after the first pronuclear division. Therefore, the thioredoxin DHD plays a critical role in early development to facilitate the switch from protamine-based sperm chromatin structures to the somatic nucleosomal chromatin.

Supplemental material is available for this article.

Received September 17, 2016; revised version accepted December 12, 2016.

Sperm DNA is compacted primarily by small arginine- and cysteine-rich proteins termed protamines (Kanippayoor et al. 2013). Thus, the structure of protamine-based chromatin of haploid sperm cells is fundamentally different from that of oligonucleosome-based somatic cell chromatin (Balhorn 1982; Braun 2001). It allows for a striking degree of nuclear compaction to maintain the paternal genome integrity and promote sperm motility (Miller et al. 2010; Rathke et al. 2014). *Drosophila* male-specific transcripts of *protamine A* (*ProtA*) and *ProtB* encode protamine-like proteins that exhibit homology with mammalian protamines and constitute the major protein component of sperm chromatin (Raja and Renkawitz-Pohl 2005; Alvi et al. 2013; Kanippayoor et al. 2013). After egg fertilization, sperm chromatin undergoes remodeling (Loppin et al. 2015), whereupon protamines are expelled from DNA by the combined action of a family of protamine chaperones (Emelyanov et al. 2014) and replaced by core histones in a process dependent on the histone chaperone HIRA (Loppin et al. 2005) and the ATP-driven motor protein CHD1 (Konev et al. 2007).

Mammalian protamines are known to undergo thiol oxidation at specific cysteine residues to form intramolecular and intermolecular disulfide bonds (Balhorn et al. 1991). It has been proposed that these covalent bonds help to stabilize the packaging of sperm DNA and contribute to its enzymatic inertness. They also likely establish a barrier to sperm chromatin remodeling and inhibit protamine removal. Consistently, chemical microinjection experiments in oocytes in vitro suggest that protamine S–S bonds need to be reversed for pronuclear formation (Perreault et al. 1984). Although it is clear that oxidation of cysteines and protamine oligomerization need to be reversed during fertilization, this process is poorly understood, and the requisite cellular machinery remains unknown. We now demonstrate that disulfide bonds within *Drosophila* protamine oligomers are specifically reduced by the embryonic thioredoxin Deadhead (DHD), and this reaction represents the obligatory initial step of sperm chromatin remodeling in vivo. Thus, the ubiquitous and evolutionarily conserved thioredoxin system (Holmgren 1985) functions in early development and is essential to convert the static sperm chromatin structures established by oligomerized protamines into the somatic nucleosomal chromatin in the nascent male pronucleus.

Results and Discussion

Upon loading on DNA, Drosophila *protamines undergo spontaneous oxidation that leads to their oligomerization*

Recombinant *Drosophila* Prot B (16.5 kDa) was purified to >95% homogeneity (Emelyanov et al. 2014). SDS-PAGE in the absence of β-mercaptoethanol (βME) reveals that it can form dimers in solution (Fig. 1A). Thus, Prot B (~0.1 mM) in mildly reducing conditions (1 mM DTT) (see the Materials and Methods) exists in equilibrium of monomeric and dimeric forms. When Prot B is further purified by size exclusion chromatography in a buffer lacking DTT, it fractionates in a single peak, in which the majority of polypeptides form dimers (Fig. 1B). In the absence of DTT, both monomers and dimers change their SDS-PAGE mobilities (Supplemental Fig. S1A), presumably due to formation of intramolecular disulfide bonds, as suggested previously for mammalian protamines (Vilfan et al. 2004). The dimerization of Prot B is also mediated by covalent disulfide bonds because SDS-PAGE of the gel filtration peak in the presence of 10 mM DTT does not reveal cross-linked dimers (Supplemental Fig. S1B). Intriguingly, the apparent molecular mass of Prot B in these chromatographic conditions remains abnormally high (>40 kDa). Prot B is purified and stored in a 500 mM NaCl-containing buffer, as we noticed that, in buffers of physiological ionic strength, the protein becomes unstable and precipitates after freezing–thawing (data not shown). When we examined its chromatographic properties in 150 mM NaCl, higher-order complexes of Prot B were disrupted, and the protein fractionated at an apparent molecular mass of

[*Keywords*: fertilization; sperm chromatin remodeling; protamine eviction; disulfide bonds; thioredoxin system]
Corresponding author: dmitry.fyodorov@einstein.yu.edu
Article published online ahead of print. Article and publication date are online at http://www.genesdev.org/cgi/doi/10.1101/gad.290916.116.

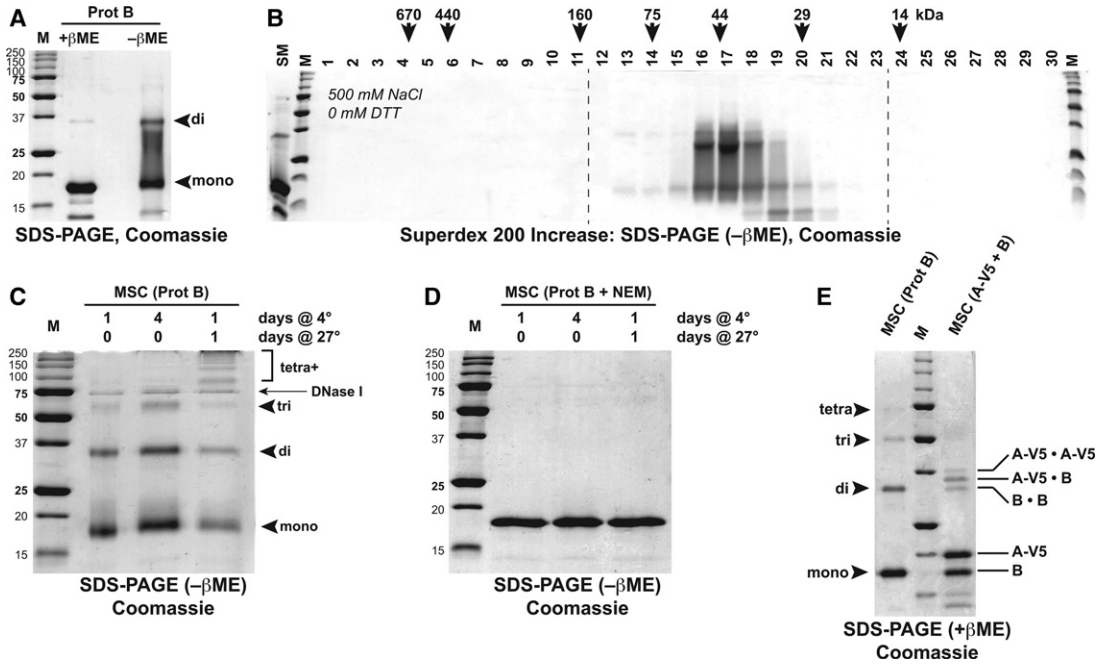

Figure 1. *Drosophila* protamines oligomerize in vitro via spontaneous formation of disulfide bonds. (*A*) SDS-PAGE of Prot B in reducing and nonreducing conditions. Purified recombinant protein (in a buffer containing 1 mM DTT) was heat-treated with or without βME, resolved on a 15% gel, and stained with Coomassie. Protein bands corresponding to molecular masses of protamine monomer and oligomers are indicated. "M" indicates molecular mass marker; marker sizes (in kilodaltons) are shown. (*B*) Size exclusion chromatography of Prot B in a nonreducing buffer. Purified recombinant protein was fractionated on Superdex 200 Increase FPLC columns in a buffer containing 500 mM NaCl and lacking DTT. Chromatographic fractions were analyzed by SDS-PAGE (in the absence of βME) and Coomassie staining. Fraction numbers and approximate positions of peaks for globular proteins of various masses (in kilodaltons) are shown *above* the gel. (SM) Starting material. (*C*) SDS-PAGE of Prot B oligomers formed upon assembly into protamine–DNA complexes (model sperm chromatin [MSC]) in vitro. MSC was assembled from plasmid DNA and Prot B by salt dialysis and incubated in a buffer containing 1 mM DTT for various times at 4°C or 27°C. DNA was degraded by an excess of DNase I (Emelyanov et al. 2014), and released proteins were analyzed in nonreducing conditions as in *A*. (*D*) SDS-PAGE of Prot B in MSC assembled from plasmid DNA and Prot B with cysteine residues blocked by N-ethylmaleimide (NEM). Analyses were performed as in *C*, except the protein was pretreated with NEM. (*E*) SDS-PAGE of homo-oligomers and hetero-oligomers of Prot A (V5-tagged) and/or Prot B (untagged) formed upon assembly into MSC in vitro. Samples were heat-treated in reducing conditions as in Supplemental Figure 1C and resolved on a 4%–20% gradient gel.

<14 kDa (Supplemental Fig. S1C). Therefore, in low salt, the predominant form of Prot B is monomeric, whereas at high ionic strength, it forms a higher-order complex. This association behavior in solution is reminiscent of that of purified core histones that exist as a mixture of H3–H4 tetramers and H2A–H2B dimers in low salt but assemble in stoichiometric octamers in high salt (Ruiz-Carrillo and Jorcano 1979). Although the resolution of size exclusion chromatography precludes a precise assignment of the molecular mass for Prot B complex in 500 mM NaCl, its composition is consistent with a homodimer (or higher). Within this complex, in buffers of low redox potential, Prot B undergoes rapid spontaneous oxidation to establish covalently linked dimers (Fig. 1B).

When we examined the oligomerization of Prot B after loading on plasmid DNA to form the model sperm chromatin (MSC) (Emelyanov et al. 2014), we also observed dimers (Fig. 1C). Moreover, prolonged incubation of MSC at 4°C or 27°C resulted in the formation of extended cross-linked oligomers (trimers, tetramers, and higher) never observed previously. *Drosophila* protamine sequences contain 10 cysteines, and thus each protamine molecule may establish more than one covalent disulfide bond and form extensive oligomeric structures. The covalent linkage was dependent on free SH moieties in cysteine residues of the protein because it was abolished in MSC assembled from Prot B in which sulfhydryl groups had been blocked with N-ethylmaleimide (NEM) (Fig. 1D). The cross-linking was very strong (possibly established through multiple S–S bonds), and even 350 mM βME failed to completely dissociate the oligomers (Supplemental Fig. S1D). In fact, in older MSC preparations stored at 4°C for several months, the oligomers became absolutely resistant to the reduction by βME, did not dissociate, and failed to enter the bottom part of the SDS-PAGE gel (Supplemental Fig. S1E). In contrast, when Prot B was processed in identical conditions but in the absence of DNA, we did not observe higher-order oligomers (Supplemental Fig. S1F).

The oligomerization of Prot B in MSC in vitro was spontaneous: It did not require enzymatic activities of protein disulfide isomerase (PDI) proteins (Bulleid and Ellgaard 2011) and thus was largely mass action-driven. Notably, MSC was prepared and all reactions were performed in mildly reducing conditions (1 mM DTT). However, 1 mM DTT is unlikely to provide an efficient competitor for the second-order chemical reaction of intermolecular cross-linking of cysteines when Prot B is loaded on the DNA, and its effective concentration is greatly increased. We also examined the ability of Prot A and Prot B to hetero-oligomerize in vitro when assembled together in MSC. We discovered that Prot A-V5 and Prot B form

both homologous and heterologous covalent cross-links with equal efficiency (Fig. 1E).

The Drosophila *thioredoxin DHD specifically reduces intermolecular disulfide bonds in protamines and facilitates their eviction from DNA*

We observed previously that, in our defined system, protamine chaperones occasionally failed to efficiently remove protamines from MSC (Emelyanov et al. 2014). It is possible that the reaction was inhibited by oxidized and oligomerized protamines that accumulated during substrate storage (Supplemental Fig. S1E). Thus, we examined the eviction of Prot B oligomers by purified TAP/p32. To this end, we used MSC assembled from V5-tagged Prot B and moderately oxidized (1 d at 27°C). The substrate was treated with a molecular excess of TAP/p32, and reaction products were fractionated by low-resolution Sephacryl S-500 gel filtration. (Simultaneously, any residual DTT was removed.) The untreated substrate peaked in early fractions, according to its high molecular mass (Fig. 2A). The monomer and higher-order protamine oligomers were apparent on the V5 Western. The presence of TAP/p32 resulted in a partial remodeling of MSC and release of Prot B-V5 from DNA into lower-molecular-mass fractions (Fig. 2B). As hypothesized, only the monomeric form of Prot B was evicted by TAP/p32, and the substrate was largely depleted of the monomers but still contained the protamine oligomers.

Crude *Drosophila* extract (S-190) has been observed to consistently outperform purified protamine chaperones in MSC remodeling reactions in vitro (Emelyanov et al. 2014). In addition to protamine chaperones, the extract may contain other activities that facilitate protamine eviction; for instance, factors that reduce disulfide bonds and disrupt protamine oligomers. Disulfide bonds are typically reduced in vivo by small proteins of the thioredoxin family (Holmgren 1985). The *Drosophila melanogaster* genome encodes at least 17 proteins with a conserved thioredoxin/thioredoxin-like fold. Of those, only two—DHD and thioredoxin 2 (TRX2)—are true small thioredoxins and are expressed in the early embryo (FlyBase). Thus, we decided to test the ability of DHD and TRX2 to interact with MSC and mediate the reduction of protamines. First, we examined whether recombinant DHD and TRX2 (Fig. 2C) bind MSC in vitro. Each V5-tagged protein was incubated with MSC assembled from untagged Prot B

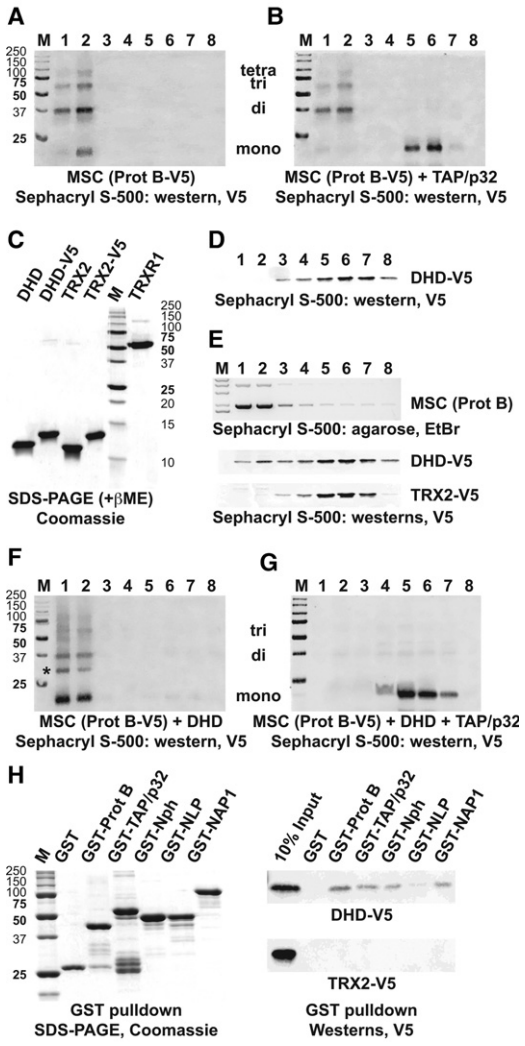

Figure 2. The thioredoxin protein DHD reduces intermolecular disulfide bonds and facilitates protamine eviction from sperm chromatin in vitro. (*A*) Size exclusion chromatography of MSC. MSC (assembled with Prot B-V5) was moderately oxidized/cross-linked (1 d at 27°C) and fractionated by gel filtration on Sephacryl S-500. Fractions were treated with DNase I as in Figure 1C and analyzed by SDS-PAGE (without βME) and immunoblotting (V5 antibody). Fraction numbers are shown at the *top*. MSC peaked in fractions 1 and 2. Positions of Prot B-V5 oligomers are indicated. (*B*) Size exclusion chromatography of MSC remodeled with protamine chaperone TAP/p32. Oxidized MSC was incubated with purified recombinant TAP/p32, fractionated, and analyzed as in *A*. Prot B-V5 monomers were removed from MSC by TAP/p32 and peaked in fractions 5 and 6. (*C*) SDS-PAGE of purified recombinant *Drosophila* thioredoxins and thioredoxin reductase. DHD, DHD-V5, thioredoxin 2 (TRX2), TRX2-V5, and TRXR1 (in sample buffer with βME) were resolved on a 15% gel and stained with Coomassie. "M" indicates molecular mass marker; marker sizes (in kilodaltons) are shown. (*D*) Size exclusion chromatography of purified DHD-V5. DHD-V5 was fractionated on Sephacryl S-500, and chromatographic fractions were analyzed by SDS-PAGE (with βME) and immunoblotting with V5 antibody. Free DHD-V5 peaks in fractions 6 and 7. (*E*) Size exclusion chromatography of purified DHD-V5 associated with MSC. DHD-V5 (*middle* panel) or TRX2-V5 (*bottom*) was incubated with MSC (assembled with untagged Prot B), fractionated, and analyzed as in *D*. (*Top*) Fractionation of MSC was examined by analyses of the fractions for the presence of plasmid DNA. MSC peaks in fractions 1 and 2, and a portion of DHD-V5 (but not TRX2-V5) cofractionates with MSC. (*F*) Size exclusion chromatography of MSC treated with DHD. Oxidized MSC was incubated with untagged DHD (supplemented with TRXR1 and NADPH), fractionated, and analyzed as in *A*. DHD partially reduces Prot B-V5 and disrupts its oligomerization. The asterisk indicates an apparent DHD-Prot B heterodimer (trapped intermediate of the reduction reaction). (*G*) Size exclusion chromatography of MSC treated with DHD and remodeled with TAP/p32. Oxidized MSC was incubated with TAP/p32, DHD, TRXR1, and NADPH; fractionated; and analyzed as in *A*. Thioredoxin and protamine chaperones synergistically disrupt Prot B-V5 cross-linking and remove it from DNA. (*H*) GST pull-down analyses of physical interactions between DHD-V5 and protamine chaperones. Physical interactions of DHD-V5 and TRX2-V5 with TAP/p32, nucleophosmin, NLP, and NAP1 were analyzed by GST pull-down. (*Left* panel) Coomassie-stained SDS-PAGE gel showing GST fusion baits in the pull-down samples. (Two *right* panels) Western blots probed with V5 antibody to detect DHD-V5 (*top*) or TRX2-V5 (*bottom*) in the pull-down and input (10%) samples. (GST alone) Negative control; (GST-Prot B) positive control.

(as in Fig. 1C) and analyzed by S-500 chromatography and V5 Western. Whereas DHD-V5 was found primarily in later chromatographic fractions (free form) (Fig. 2D,E), some of the protein also cofractionated with MSC (Fig. 2E), indicating their physical association. The interaction was specific to DHD-V5, since TRX2-V5 failed to interact with MSC (Fig. 2E). Also, the binding strongly depended on the presence of Prot B in the substrate because DHD-V5 exhibited a much weaker interaction with the naked plasmid DNA (Supplemental Fig. S2A).

We then tested whether DHD can reduce oxidized forms of Prot B and reverse its disulfide bond-dependent oligomerization in MSC. The MSC substrate (Prot B-V5 as in Fig. 2A) was treated with untagged DHD in a reaction supplemented with substoichiometric embryonic thioredoxin reductase, TRXR1 (Fig. 2C), and 0.5 mM NADPH to activate DHD. Gel filtration and Western blotting revealed that DHD can partially disrupt protamine oligomers (Fig. 2, cf. F and A): The apparent abundance of Prot B-V5 monomer was greatly increased at the expense of dimers and other oligomers in the MSC factions. However, the association of Prot B-V5 (including monomers) with the DNA was not affected. Thus, DHD can mediate the reduction of Prot B-V5 but does not itself promote its eviction from MSC. When TAP/p32 was added to a similar reaction, the MSC was completely dissociated (Fig. 2, cf. G and B). The entirety of Prot B-V5 was evicted from DNA and fractionated in a monomeric form in the "released protamine" fractions. The products of similar reactions were also fractionated by high-resolution chromatography on Superdex 200 Increase (Supplemental Fig. S2B) to reveal details of a putative molecular mechanism. Apparently, upon reducing intermolecular disulfide bonds by DHD, Prot B monomers become available for binding and eviction from DNA in a complex with TAP/p32.

In contrast, when MSC was assembled from NEM-treated Prot B-V5 (as in Fig. 1D) that cannot oligomerize, its eviction from DNA was efficiently mediated by TAP/p32 alone in the absence of DHD (Supplemental Fig. S2C). The DHD-dependent remodeling of MSC required NADPH and TRXR1, the components of the reconstitution system (Supplemental Fig. S2D). Finally, consistent with its inability to physically interact with MSC, TRX2 could not substitute DHD and did not reduce protamine disulfide bonds or stimulate sperm chromatin remodeling in vitro (Supplemental Fig. S2D). We also tested whether DHD can reduce substrates that contained Prot A. To this end, we used MSC assembled from Prot A-V5 and Prot B (as in Fig. 1E) and treated it with various combinations of TAP/p32 and DHD (+reconstitution system). We discovered that DHD also strongly stimulated the eviction of Prot A-V5 (Supplemental Fig. S2E). Thus, DHD can reduce both *Drosophila* protamines in vitro and functions as an essential and specific cofactor that facilitates remodeling of sperm chromatin that contains disulfide bond-linked protamine molecules.

DHD and TAP/p32 exhibit a strong synergy in MSC remodeling in vitro. Not only does DHD stimulate protamine eviction by TAP/p32, but the presence of TAP/p32 also enhances the conversion of protamines to monomers by DHD (Fig. 2, cf. F and G). The cooperative effect may result from a relaxation of steric hindrance within the substrate (MSC), which becomes more accessible to DHD upon the gradual release of protamines by the chaperone. Additionally, it is possible that DHD and TAP/p32 physically interact to facilitate each other's tethering to MSC and increase the reaction rate. We examined the binding between DHD-V5 and GST-TAP/p32 by GST pull-down and discovered that they do in fact interact (Fig. 2H). Importantly, DHD-V5 did not bind GST alone but interacted with GST-Prot B, consistent with its specific association with Prot B-containing MSC (Fig. 2E). DHD also interacted with other protamine chaperones (NAP1, NLP, and Nph) (Fig. 2H). As controls, Prot A-V5 exhibited promiscuous binding to all protamine chaperones (Supplemental Fig. S2F), whereas Prot B-V5 strongly associated only with GST-TAP/p32, consistent with earlier findings (Emelyanov et al. 2014). The interactions of DHD-V5 with protamine chaperones were specific and not shared by TRX2-V5, which failed to bind to any of the tested GST fusions in identical conditions (Fig. 2H). The observation of DHD-TAP/p32 binding was also confirmed by glycerol gradient cosedimentation (Supplemental Fig. S2G). Thus, DHD binds TAP/p32 (and other protamine chaperones), and the physical interaction may play an important role in their cooperative function in sperm chromatin remodeling (Fig. 2G).

Our biochemical analyses reveal crucial details of the molecular transitions (summarized in Supplemental Fig. S3) that protamine molecules undergo during deposition on/eviction from DNA in vitro. These details likely reflect many of the elementary mechanisms of protamine metabolism in vivo. For instance, although one report has implicated a mammalian selenoprotein, snGPx, in thiol cross-linking of protamines in sperm cells (Pfeifer et al. 2001), it is possible that protamines can also undergo oligomerization in the absence of specialized PDIs via spontaneous, mass action-driven oxidation of cysteines due to a dramatically elevated effective concentration. Importantly, our model also predicts that the embryonic thioredoxin DHD should be required for sperm chromatin remodeling in a fertilized egg.

Drosophila *DHD is required for sperm chromatin remodeling in vivo*

The amorphic mutant of *Drosophila deadhead* (*dhd*) has been described (Salz et al. 1994). *dhd* is not essential for adult viability but is recessive maternal effect lethal: The majority of eggs laid by homozygous females is fertilized but fails to initiate development. To test whether DHD affects sperm decondensation and protamine eviction, we crossed homozygous *dhd* mothers with fathers that carry transgenes expressing *eGFP*-tagged *ProtB* and *don juan* (*dj*) that encode the major components of sperm heads and tails, respectively (Santel et al. 1997; Raja and Renkawitz-Pohl 2005). Heterozygous *dhd/FM7* mothers were used in control crosses. We discovered that *dhd* embryos were completely incapable of processing sperm chromatin. Microscopic analyses revealed that the majority of 0- to 4-h embryos (>60% of the total scored) was fertilized and contained GFP-labeled sperm. Importantly, they failed to remove Prot B from sperm heads, which remained fully compacted (Fig. 3A). In most of the embryos (~55% of the total), the female pronuclei underwent one haploid mitosis but terminated further divisions. The sperm heads did not specifically migrate to the middle of the embryo but rather assumed random positions within the egg. Figure 3B presents a condensed sperm head that is positioned in the same focal plane as the divided female

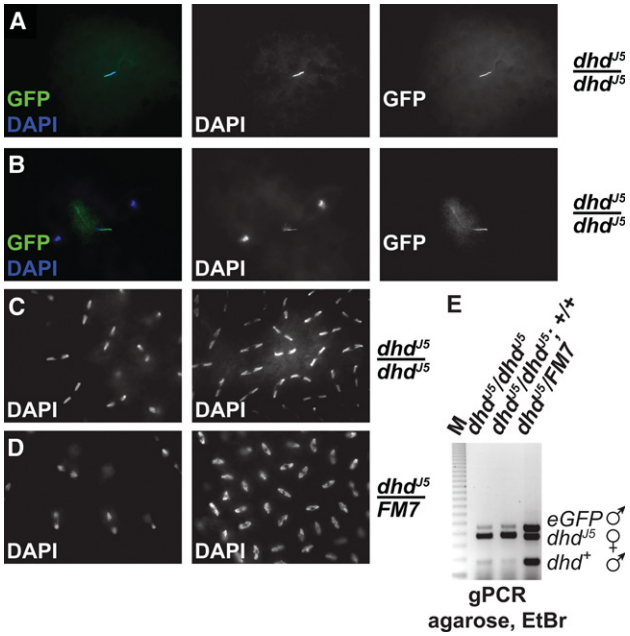

Figure 3. *Drosophila dhd* is required for sperm chromatin remodeling during fertilization. (*A*) The failure to decondense sperm chromatin in a homozygous *dhd* mutant embryo. Homozygous mutant dhd^{J5} females were crossed to males carrying *ProtB-eGFP* and *dj-GFP* transgenes. Embryos were collected (0–4 h after egg deposition [AED]), fixed, stained with DAPI, and examined microscopically for DAPI (blue) and GFP (green) fluorescence. Both the sperm head (*ProtB-eGFP*) and tail (*dj-GFP*) are labeled with GFP. (*B*) Persistent condensed sperm chromatin during the apposition stage of early homozygous *dhd* mutant embryos. Two female pronuclei that have undergone one round of haploid mitosis and a Prot B-eGFP-containing sperm cell in the same focal plane are shown. (*C*) Haploid mitoses in homozygous *dhd* mutant embryos. dhd^{J5} embryos were collected and stained with DAPI as in *A* and *B*. Rare (~5%) escapers that developed beyond the apposition stage underwent haploid mitoses. Shown are anaphases and division cycles 10 (*left*) and 12 (*right*). (*D*) Normal diploid mitoses in heterozygous dhd^{J5}/*FM7* embryos. The appearance of anaphase chromosomes in control embryos collected and analyzed as in *C*. (*E*) Genomic PCR analyses in homozygous and heterozygous *dhd* embryos. Crosses were performed between males carrying *P{ProtB-eGFP}* and *P{dj-GFP}* insertions and females of different genotypes as indicated at the *top*. (dhd^{J5}/dhd^{J5} and dhd^{J5}/dhd^{J5}; +/+ females were produced by inter se crosses of dhd^{J5}/*FM7* and dhd^{J5}/dhd^{J5}; +/*CyO, P{dhd*$^+$*}* parents, respectively.) Embryos were collected as in *A*, and the propagation of genomic material from mothers (♀, dhd^{J5}) and fathers (♂, dhd^+ and *eGFP*) was examined by multiplex PCR amplification of genomic DNA. Only female DNA was efficiently amplified in *dhd/dhd* embryos. The scarce male-specific PCR products (dhd^+ and *eGFP*) were likely amplified from minute amounts of sperm DNA present in fertilized eggs. "M" indicates a 123-base-pair DNA ladder.

pronuclei. Similar phenotypes are revealed by DAPI staining of embryos produced in a cross of homozygous *dhd* mothers and wild-type fathers (Supplemental Fig. S4). In contrast, *dhd/FM7* embryos did not exhibit any developmental defects. Also, we could not detect any Prot B-eGFP-labeled sperm heads after inspecting >2000 fertilized heterozygous embryos, consistent with an extremely fast (within minutes and, frequently, before egg deposition) sperm decondensation and protamine eviction during normal development (Loppin et al. 2015).

Occasionally, *dhd/dhd* embryos (~5% of the total) entered syncytial divisions but aborted their development prior to cellularization. Although we could not detect persistent sperm cells in these syncytial embryos, other evidence indicated that they did not remodel sperm chromatin or form the male pronucleus. First, the appearance of anaphase chromosomes suggested a haploid DNA content (Fig. 3, cf. C for *dhd/dhd* and D for the heterozygous control). Furthermore, PCR analyses of maternal- and paternal-derived sequences in the genomic DNA of *dhd* embryos exposed a very strong overabundance of maternal DNA (Fig. 3E). The aborted development of gynogenetic haploid embryos in the *dhd* mutant is similar to that in mutants of *ssm*, *yem*, and *Chd1*, which encode the HIRA–YEM complex and CHD1, the factors required for nucleosome assembly in the male pronucleus (Loppin et al. 2005; Konev et al. 2007; Orsi et al. 2013). However, in contrast to *dhd* mutation, *ssm*, *yem*, and *Chd1* mutations lead to the vast majority of embryos entering haploid syncytial divisions. Therefore, although DHD is clearly required for sperm chromatin remodeling in vivo, it may also be involved in other embryonic functions, such as regulation of DNA synthesis or S-phase initiation during preblastoderm mitosis, as proposed previously (Salz et al. 1994; Pellicena-Palle et al. 1997).

In metazoan development, nuclear DNA undergoes dramatic differentiation-dependent, activity-dependent, and cell cycle-dependent transitions that alter the composition, distribution, and modification status of associated proteins. We demonstrate that *Drosophila* sperm chromatin compaction involves oligomerization of protamines via intermolecular disulfide bridges. To convert the condensed, static, and metabolically inert paternal chromatin into a transcriptionally and otherwise enzymatically competent somatic cell chromatin, the embryo expresses a network of specialized proteins, which includes the thioredoxin DHD and protamine chaperones. Synergistically, they reverse the protamine oligomerization and remove them from DNA during fertilization. This network of physically interacting proteins plays an essential role in early embryonic development. Metazoans exhibit a strong similarity in amino acid content (cysteine enrichment) and secondary structure of protamines (intramolecular and intermolecular disulfide bonds) as well as primary structures of protamine chaperones and various thioredoxins. Thus, the function of the thioredoxin system in sperm chromatin remodeling is likely conserved in evolution.

Materials and methods

Recombinant proteins

Bacterial expression constructs for purification of untagged or V5-tagged Prot A and Prot B and His_6-tagged TAP/p32 have been described (Emelyanov et al. 2014). Similar constructs for purification of thioredoxins DHD, DHD-V5, TRX2, and TRX2-V5; thioredoxin reductase TRXR1; GST-His_6; GST-Prot B-His_6; GST-NLP-His_6; GST-Nph-His_6; and GST-TAP/p32-His_6 were prepared by PCR and molecular cloning. See the Supplemental Material for details of cloning, expression in *Escherichia coli*, and purification.

Superdex 200 Increase size exclusion chromatography

Purified recombinant Prot B was fractionated in different chromatographic buffers (HEG + 0.02% NP-40, 0.2 mM PMSF, 0.5 mM benzamidine, 0 or 10 mM DTT, 150 or 500 mM NaCl) on an ~24-mL Superdex 200 Increase 10/300 GL column on AKTA FPLC (GE Life Sciences). Typically, 0.5-mL starting material samples containing ~0.5 mg of protein in a buffer with the NaCl concentration equal to that of the chromatographic buffer were injected on the column and fractionated isocratically at 0.4 mL/

min, and 0.5-mL fractions corresponding to 0.3–1.0 column volumes were collected and analyzed by SDS-PAGE (in the absence of βME) and Coomassie staining. Molecular weights of fractionating proteins were assigned based on the column calibration by the manufacturer (GE Life Sciences).

MSC remodeling in vitro

To reduce disulfide bonds in DNA-bound protamines in vitro, we used purified recombinant *Drosophila* embryonic thioredoxin DHD (Pellicena-Palle et al. 1997) in a molar excess relative to protamine monomers (~2:1). To activate (reduce) DHD, the reactions were also supplemented with a reconstitution system comprising substoichiometric amounts (1:200 to 1:100 molar ratio to DHD) of *Drosophila* embryonic thioredoxin reductase TRXR1 (Cheng et al. 2007) and 0.5 mM NADPH electron donor (at least 30:1 molar ratio to DHD). The association of protamines with and their release from DNA was examined by size exclusion chromatography and Western with anti-V5 antibody as described (Emelyanov et al. 2014). See the Supplemental Material for experimental details.

Protein–MSC and protein–protein interaction studies

Sephacryl S-500 chromatography was also used to examine physical interactions between DHD and MSC, whereas GST pull-down assays and glycerol gradient cosedimentation analyses were used for studies of physical interactions among recombinant thioredoxins, protamines, and protamine chaperones. See the Supplemental Material for details of the protocols.

Staining of Drosophila *embryos*

For cytological analyses using DAPI and GFP autofluorescence, embryos were collected 0–4 h after egg deposition (AED), stored for up to 6 h at 4° C, dechorionated, and fixed in methanol as described (Konev et al. 2007). The embryos were mounted in VectaShield (Vector Laboratories) with 1 µg/mL DAPI and observed under a Zeiss Axiovert 200M. For each experiment, >2000 embryos were examined. Images were processed using IP Lab and Photoshop.

Acknowledgments

We are grateful to Helen Salz for fly stocks. We thank Elena Vershilova for expert technical assistance, and Konstantin Beirit, Matthew Gamble, James Kadonaga, Michael-Christopher Keogh, Alexander Konev, and Arthur Skoultchi for helpful discussions and critical reading of the manuscript. This work was supported by a grant from the National Institutes of Health (GM074233) to D.V.F.

References

Alvi ZA, Chu TC, Schawaroch V, Klaus AV. 2013. Protamine-like proteins in 12 sequenced species of *Drosophila*. *Protein Pept Lett* **20:** 17–35.

Balhorn R. 1982. A model for the structure of chromatin in mammalian sperm. *J Cell Biol* **93:** 298–305.

Balhorn R, Corzett M, Mazrimas J, Watkins B. 1991. Identification of bull protamine disulfides. *Biochemistry* **30:** 175–181.

Braun RE. 2001. Packaging paternal chromosomes with protamine. *Nat Genet* **28:** 10–12.

Bulleid NJ, Ellgaard L. 2011. Multiple ways to make disulfides. *Trends Biochem Sci* **36:** 485–492.

Cheng Z, Arscott LD, Ballou DP, Williams CH Jr. 2007. The relationship of the redox potentials of thioredoxin and thioredoxin reductase from *Drosophila melanogaster* to the enzymatic mechanism: reduced thioredoxin is the reductant of glutathione in *Drosophila*. *Biochemistry* **46:** 7875–7885.

Emelyanov AV, Rabbani J, Mehta M, Vershilova E, Keogh MC, Fyodorov DV. 2014. *Drosophila* TAP/p32 is a core histone chaperone that cooperates with NAP-1, NLP, and nucleophosmin in sperm chromatin remodeling during fertilization. *Genes Dev* **28:** 2027–2040.

Holmgren A. 1985. Thioredoxin. *Annl Rev Biochem* **54:** 237–271.

Kanippayoor RL, Alpern JH, Moehring AJ. 2013. Protamines and spermatogenesis in *Drosophila* and *Homo sapiens*: a comparative analysis. *Spermatogenesis* **3:** e24376.

Konev AY, Tribus M, Park SY, Podhraski V, Lim CY, Emelyanov AV, Vershilova E, Pirrotta V, Kadonaga JT, Lusser A, et al. 2007. CHD1 motor protein is required for deposition of histone variant H3.3 into chromatin in vivo. *Science* **317:** 1087–1090.

Loppin B, Bonnefoy E, Anselme C, Laurençon A, Karr TL, Couble P. 2005. The histone H3.3 chaperone HIRA is essential for chromatin assembly in the male pronucleus. *Nature* **437:** 1386–1390.

Loppin B, Dubruille R, Horard B. 2015. The intimate genetics of *Drosophila* fertilization. *Open Biol* **5** pii: 150076.

Miller D, Brinkworth M, Iles D. 2010. Paternal DNA packaging in spermatozoa: more than the sum of its parts? DNA, histones, protamines and epigenetics. *Reproduction* **139:** 287–301.

Orsi GA, Algazeery A, Meyer RE, Capri M, Sapey-Triomphe LM, Horard B, Gruffat H, Couble P, Ait-Ahmed O, Loppin B. 2013. *Drosophila* Yemanuclein and HIRA cooperate for de novo assembly of H3.3-containing nucleosomes in the male pronucleus. *PLoS Genet* **9:** e1003285.

Pellicena-Palle A, Stitzinger SM, Salz HK. 1997. The function of the *Drosophila* thioredoxin homologue encoded by the *deadhead* gene is redox-dependent and blocks the initiation of development but not DNA synthesis. *Mech Dev* **62:** 61–65.

Perreault SD, Wolff RA, Zirkin BR. 1984. The role of disulfide bond reduction during mammalian sperm nuclear decondensation in vivo. *Dev Biol* **101:** 160–167.

Pfeifer H, Conrad M, Roethlein D, Kyriakopoulos A, Brielmeier M, Bornkamm GW, Behne D. 2001. Identification of a specific sperm nuclei selenoenzyme necessary for protamine thiol cross-linking during sperm maturation. *FASEB J* **15:** 1236–1238.

Raja SJ, Renkawitz-Pohl R. 2005. Replacement by *Drosophila melanogaster* protamines and Mst77F of histones during chromatin condensation in late spermatids and role of *sésame* in the removal of these proteins from the male pronucleus. *Mol Cell Biol* **25:** 6165–6177.

Rathke C, Baarends WM, Awe S, Renkawitz-Pohl R. 2014. Chromatin dynamics during spermiogenesis. *Biochim Biophys Acta* **1839:** 155–168.

Ruiz-Carrillo A, Jorcano JL. 1979. An octamer of core histones in solution: central role of the H3–H4 tetramer in the self-assembly. *Biochemistry* **18:** 760–768.

Salz HK, Flickinger TW, Mittendorf E, Pellicena-Palle A, Petschek JP, Albrecht EB. 1994. The *Drosophila* maternal effect locus *deadhead* encodes a thioredoxin homolog required for female meiosis and early embryonic development. *Genetics* **136:** 1075–1086.

Santel A, Winhauer T, Blumer N, Renkawitz-Pohl R. 1997. The *Drosophila don juan* (*dj*) gene encodes a novel sperm specific protein component characterized by an unusual domain of a repetitive amino acid motif. *Mech Dev* **64:** 19–30.

Vilfan ID, Conwell CC, Hud NV. 2004. Formation of native-like mammalian sperm cell chromatin with folded bull protamine. *J Biol Chem* **279:** 20088–20095.